ELSEVIER

European Journal of Cancer 40 (2004) 2175–2183

European Journal of Cancer

www.ejconline.com

5′CpG island hypermethylation and aberrant transcript splicing both contribute to the inactivation of the *FHIT* gene in resected non-small cell lung cancer☆

Ching Tzao [a,1], Hui-Yuan Tsai [b,1], Jung-Ta Chen [c], Chih-Yi Chen [d], Yi-Ching Wang [b,*]

[a] *Division of Thoracic Surgery, Tri-Service General Hospital, National Taiwan Normal University, Taipei, Taiwan, ROC*
[b] *Department of Life Sciences, National Taiwan Normal University, No. 88, Sec. 4, Tingchou Rd., Taipei 116, Taiwan, ROC*
[c] *Department of Pathology, Taichung Veterans General Hospital, Taichung, Taiwan, ROC*
[d] *Division of Thoracic Surgery, Taichung Veterans General Hospital, Taichung, Taiwan, ROC*

Received 19 February 2004; received in revised form 25 May 2004; accepted 22 June 2004
Available online 19 August 2004

Abstract

The relative contribution of promoter hypermethylation and aberrant splicing to the inactivation of the fragile histidine triad (*FHIT*) gene is unclear. Using genetic and epigenetic analyses, the current investigation examines the loss of protein and mRNA expression, and 5′CpG hypermethylation and allelic imbalance of the *FHIT* gene in a series of 129 non-small cell lung cancer (NSCLC) samples, in parallel with clinicopathological analyses. We found that 50% of NSCLC patients had aberrant protein expression, which was more frequent in squamous cell carcinomas (SQ) (69%) than in adenocarcinomas (AD) (28%) ($P<0.0001$). 5′CpG hypermethylation of *FHIT* was identified in 31% of patients. Abnormally-sized *FHIT* transcripts were also observed in 24% of patients and were attributed to various exonic deletions, mainly in the region of exons 4–8. Allelic imbalance of the *FHIT* locus and its correlation with the status of Fhit expression, 5′CpG hypermethylation, and aberrant splicing, indicated that biallelic inactivation of Fhit expression could be induced by 5′CpG hypermethylation of one allele and alternative splicing in the other allele. Moreover, an 83% concordance in the methylation status of *FHIT* was demonstrated between 12 samples of bronchial precancerous lesions taken before surgery and their matched resected tumours. Our data suggest that *FHIT* 5′CpG hypermethylation and splicing alterations are both predominant mechanisms involved in the aberrant expression of the *FHIT* gene, and that *FHIT* 5′CpG methylation may be potentially used as a supplemental detection marker for NSCLC.

Keywords: *FHIT* gene; 5′CpG hypermethylation; Alternative splicing; LOH; NSCLC; Bronchial lesions

1. Introduction

Lung cancer is one of the most common malignancies in the world and is the leading cause of cancer-related deaths in industrial countries. It is generally believed that carcinogenesis is a multistep process involving the activation of oncogenes or the inactivation of tumour suppressor genes. Genetic analysis of tumour suppressor genes may reveal the molecular mechanisms involved in tumorigenesis. A proposed tumour suppressor gene, the

Abbreviations: FHIT; fragile histidine triad; NSCLC; non-small cell lung cancer; AD; adenocarcinoma; SQ; squamous cell carcinoma; AS; adenosquamous cell carcinoma; LC; large-cell carcinomas; IHC; immunohistochemistry; RT-PCR; reverse transcriptase-polymerase chain reaction; MSP; methylation-specific PCR; LOH; loss of heterozygosity.

☆ This work was supported in part by Grants NSC 91-3112-P-003-001 and NHRI93A1-NSCLC06-5 from the National Science Council (The Executive Yuan, Republic of China).

* Corresponding author. Tel.: +886-2-29336876x373; fax: +886-2-29312904.
E-mail address: t43017@cc.ntnu.edu.tw (Y.-C. Wang).

[1] These authors contributed equally to this work.

0959-8049/$ - see front matter © 2004 Elsevier Ltd. All rights reserved.
doi:10.1016/j.ejca.2004.06.022

fragile histidine triad (*FHIT*) gene, was cloned by Ohta and Colleagues in 1996 [1], and was shown to occur in *FRA3B* in chromosomal band 3p14.2, one of the most active common fragile sites in the human genome [2,3]. The *FRA3B* locus flanks the first *FHIT* coding exon, an exon that is frequently targeted by homozygous deletions in cancer-derived cell lines [3,4]. The *FHIT* alterations reported in various cancers have demonstrated features that are not usually attributed to classical tumour suppressor genes, such as a lack of point mutations and the presence of associated wild-type transcripts [5]. Furthermore, the introduction of a wild-type *FHIT* expression construct into HeLa cells lacking endogenous expression of Fhit protein did not suppress tumorigenicity in animals [6]. However, mice carrying one or two inactivated *FHIT* alleles are highly susceptible to tumour induction by carcinogen treatment [7], which can be inhibited by recombinant viral *FHIT* gene delivery [8,9]. Recent evidence also supports a role for *FHIT* as a tumour suppressor gene in different epithelial cancers, such as prostate, breast, ovarian and oesophageal cancers [10–13].

Alteration of the *FHIT* gene or protein is frequently found in lung cancer. Various loss of heterozygosity (LOH) assays have indicated a high frequency of allele loss in the *FHIT* gene at 3p14.2 [4,14–16] and patients with LOH have a tendency for poor survival [17]. A lack of Fhit protein is also found in primary lung tumours and cell lines [18,19], and is associated with smoking [20]. However, contrary results have been reported when loss of Fhit expression has been correlated with abnormal *FHIT* transcripts [18,21]. Sequence analysis revealed that abnormal *FHIT* transcripts are mainly due to abnormal splicing and processing of the transcripts [21] and that genomic mutation occurs rarely in the *FHIT* gene [15]. In data published to date, only one report shows *FHIT* methylation, in 37% of primary NSCLC and in 65% of lung cancer cell lines [22]. It is noteworthy that changes in the *FHIT* gene or protein can be detected in bronchial brushing [22] and bronchial lesions [20,23] from chronic smokers without cancer, indicating that deregulation of *FHIT* may be an early event in the pathogenesis of lung cancer.

The frequency and mechanisms of *FHIT* gene inactivation and their correlation with loss of protein expression in NSCLC vary between different studies. Furthermore, data concerning the relative contribution of promoter hypermethylation and aberrant splicing to the *FHIT* gene inactivation have never been documented in the same series of NSCLC. To elucidate the possible mechanisms involved in *FHIT* changes in NSCLC tumorigenesis, we performed a comprehensive genetic and epigenetic study of the *FHIT* status in a series of 129 NSCLC tumours and 12 matched bronchial samples taken before surgery.

2. Materials and methods

2.1. Patients and sample preparation

Tissues were collected after obtaining appropriate institutional review board permission and informed consent from the recruited patients. Surgically resected tumour samples from 129 patients with NSCLC were collected between 1993 and 2000. Of these patients, 54 had adenocarcinoma (AD), 68 had squamous carcinoma (SQ), three had adenosquamous cell carcinoma (AS), and four had large-cell carcinoma (LC). Twelve patients underwent fiber-optic bronchoscopy 1–6 months before surgery to obtain the bronchial biopsy samples. Pathological examination revealed hyperplasia and metaplasia in all patients. Mild dysplasia and moderate dysplasia occurred in 3 of the 12 cases. The histology of the tumour types and their stages were determined according to the World Health Organization (WHO) classification and the TNM system, respectively. Information on the age, gender, and smoking history of the patients with lung cancer was obtained from hospital records.

Surgically resected tumour samples were immediately snap-frozen and subsequently stored in liquid nitrogen. For the methylation assay, genomic DNA was prepared using proteinase K digestion and phenol–chloroform extraction, followed by ethanol precipitation. For LOH analysis, samples were microdissected to recover only tumour tissue from four 5-μm serial sections containing formalin-fixed, paraffin-embedded tumours and normal lung. A 25-gauge needle attached to a tuberculin syringe was used to remove the tumour cells under a dissecting microscope. After samples were dewaxed in xylene, genomic DNA was extracted according to the standard methods described above. For the RNA expression assay, total RNA was prepared from matched pairs of primary tumours and nearby normal lung tissues, using Trizol reagent (Invitrogen, Carlsbad, CA). cDNA was synthesised using SuperScript™ reverse transcriptase (Invitrogen) with the protocols provided by the manufacturer.

2.2. Immunohistochemical analysis

Paraffin blocks of tumours were cut into 5-μm sections and then processed using standard techniques. Sections were deparaffinised with xylene, then rehydrated with increasing concentrations of ethanol. Antigen retrieval was performed by microwaving the tissue sections in 10 mM sodium citrate buffer (pH 6.0) five times for 2 min each, followed by the inhibition of endogenous peroxidase activity. Sections were incubated for 2 h at room temperature with polyclonal rabbit anti-Fhit antibody (clone 18-0219; Zymed Laboratories, South San Francisco, CA) diluted 1:200, then with biotinylated goat anti-rabbit antibody (DAKO, Carpinte-

ria, CA). Sections were then incubated for 20 min with streptavidin-conjugated horseradish peroxidase and Fhit protein was visualised after a final incubation for 10 min with diaminobenzidene as the chromogen (DAKO). Sections were counterstained with haematoxylin (Zymed Laboratories), mounted with Clearmount (Zymed Laboratories), and covered with coverslips.

The normal staining pattern for Fhit was cytoplasmic. All sections were examined at 200× magnification with a light microscope. Staining intensity was scored by two observers who were unaware of the status of the sections being examined. A scoring system was used [20] based on the percentage of cells stained (<10%, +1; 10–50%, +2; >50%, +3). Tumour cells that scored +1 in the presence of non-neoplastic cells and infiltrating lymphocytes with cytoplasmic staining were considered to have a marked reduction or absence of Fhit protein expression.

2.3. Multiplex reverse transcriptase-polymerase chain reaction (RT-PCR) and cDNA sequencing

RNA was extracted and 98 samples had qualified RNA for further analysis. *FHIT* mRNA expression was assayed in a multiplex RT-PCR analysis using the β-*actin* gene as an internal control. The coding regions of exons 3–10 of the *FHIT* gene were amplified using primers 5U1 and 3D1 described by Tanaka and colleagues [13]. Reactions were carried out in a volume of 25 μl with 5 μl cDNA and 0.2 pmol primers on a DNA thermal cycler. PCR was performed for 40 cycles with an annealing temperature of 58 °C. A second PCR using 1/10 of the first PCR product was performed with nested primers. The number of cycles and the amount of primers and the cDNA used were determined to provide quantitative amplification during multiplex RT-PCR. To quantify the relative levels of gene expression in the multiplex RT-PCR assay, the value for the internal standard (β-*actin*) in each test tube was used as the baseline value for gene expression in that sample, and a relative value was calculated for each target *FHIT* transcript amplified from each tumour and matched normal sample. Tumour cells that exhibited mRNA expression below 50% of that of normal cells were deemed to have an abnormal pattern. These values were then used to compare expression across the samples tested. Abnormal cDNA fragments detected in RT-PCR assays were eluted and purified with Qiaex II Gel Extraction Kit (Qiagen, Valencia, CA), then sequenced using an ABI 377 automatic sequencer (PE Applied Biosystems, Foster City, CA) using the 5U1 primer, as described previously in [13].

2.4. Methylation-specific PCR and bisulphite genomic sequencing

Samples for the methylation assay were selected on the basis that they comprised more than 70% tumour tissue when observed within each of the resected tissue sections at low-power (100×) magnification under a light microscope. Therefore, the methylation assay was performed with 91 samples. The methylation status in the exon 1 region of the *FHIT* gene was determined by chemical treatment with sodium bisulphite and subsequent methylation-specific PCR (MSP) analysis. Primers for the methylated *FHIT* reaction were the D-SQ primer (forward) described by Tanaka and colleagues in [13] and 5′-CGTAAACGACGCCGACCCCACTA-3′ (reverse); and primers for the unmethylated *FHIT* reaction were the D-SQ primer (forward) and 5′-CATAAACAACACCAACCCCACTA-3′ (reverse). PCR was performed for 45 cycles with annealing temperatures of 63 and 68 °C for unmethylated and methylated reactions, respectively, using 100 ng bisulphite-modified DNA. DNA from BES6 normal bronchial cell line and H1299 lung cancer cell line was included in each assay to serve as unmethylated and methylated controls, respectively. Negative control samples lacking DNA were also included for each set of PCR. In addition, DNA of 26 normal lung tissues from NSCLC patients was examined before performing the assay for the 91 tumour samples from the patients. *FHIT* hypermethylation was defined as the amplification of more aberrantly methylated products than unmethylated products from the tumour sample. The sequencing primers for the analysis of methylated and unmethylated *FHIT* alleles were the corresponding MSP forward primers described above. The samples were sequenced using an ABI 377 automatic sequencer (PE Applied Biosystems).

2.5. Loss of heterozygosity analysis

Genomic DNA (20 ng) from normal lung cells or the microdissected tumour samples from 64 patients were used for each PCR analysis. PCRs were conducted in a 10 μl volume using 0.05 μM fluorescently labelled and unlabelled primers for the D3S1234 dinucleotide microsatellite marker (located in intron 3 of the *FHIT* gene), 2.5 mM $MgCl_2$, and 0.5 U AmpliTaq DNA polymerase (PE Applied Biosystems), with protocols provided by the manufacturer (PE Applied Biosystems). The primer sequences were obtained from Research Genetics (Huntsville, AL). PCR products were mixed with fluorescent molecular weight markers for subsequent electrophoresis in an ABI 377 automatic sequencer. Allele sizes were determined using GeneScan Analysis version 3.0 and Genotyper version 2.1 software. The allelic ratio was calculated as (T1/T2)/(N1/N2), the ratio of area values for tumour (T) versus normal (N) alleles. LOH was defined as an allelic ratio above 2.0 or below 0.5.

2.6. Statistical analysis

Pearson's χ^2 test was used to compare the frequency of *FHIT* alterations in NSCLC patients with different characteristics, including gender and smoking status, and various clinicopathological parameters, such as tumour type and tumour stage. The comparison of age distributions between patients with and without changes in *FHIT* was analysed with a two-sample *t*-test.

3. Results

3.1. Fhit protein expression in primary NSCLC tumours and its correlation with clinical parameters in NSCLC patients

Immunohistochemical staining was performed on 129 tumour samples. Staining within the cytoplasm of tumour cells was considered positive. Sixty-four lung tumours showed staining of moderate to strong intensity (Figs. 1A and B). The remaining 65 lung cancers (50%) showed aberrant expression of Fhit protein, characterised by a low level or complete absence of cytoplasmic staining (Figs. 1C and D). Chi-squared analysis indicated a highly significant correlation between aberrant Fhit expression and histological type, recorded as negative staining in 69% (47/68) of NSCLC with SQ compared with 28% (15/54) of NSCLC with AD ($P<0.0001$) (Table 1).

3.2. FHIT mRNA expression and its correlation with clinical parameters of NSCLC patients

RNA with high quality for multiplex RT-PCR analysis was extracted from 98 tumours (Fig. 2A). Decreased or aberrant *FHIT* transcripts were shown by RT-PCR to occur in 38 tumours (39%) (Table 1). Chi-squared analysis showed that low mRNA expression appeared to be more frequent in SQ (49%) than in AD (30%), although the statistical significance of this difference was borderline ($P=0.068$) (Table 1). The mutational spectrum was examined in the 24 samples with abnormally-sized *FHIT* transcripts, using cDNA sequencing. Aberrant bands were mainly attributed to the deletion of exons 4, 5, 6, 7 and 8 of *FHIT* (Fig. 2B). In addition, 19 of the normal lung tissues showed a faint additional band of an aberrant size. However, in contrast to data from tumours, no abnormal protein expression in the normal lung tissue was seen in any of the cases including

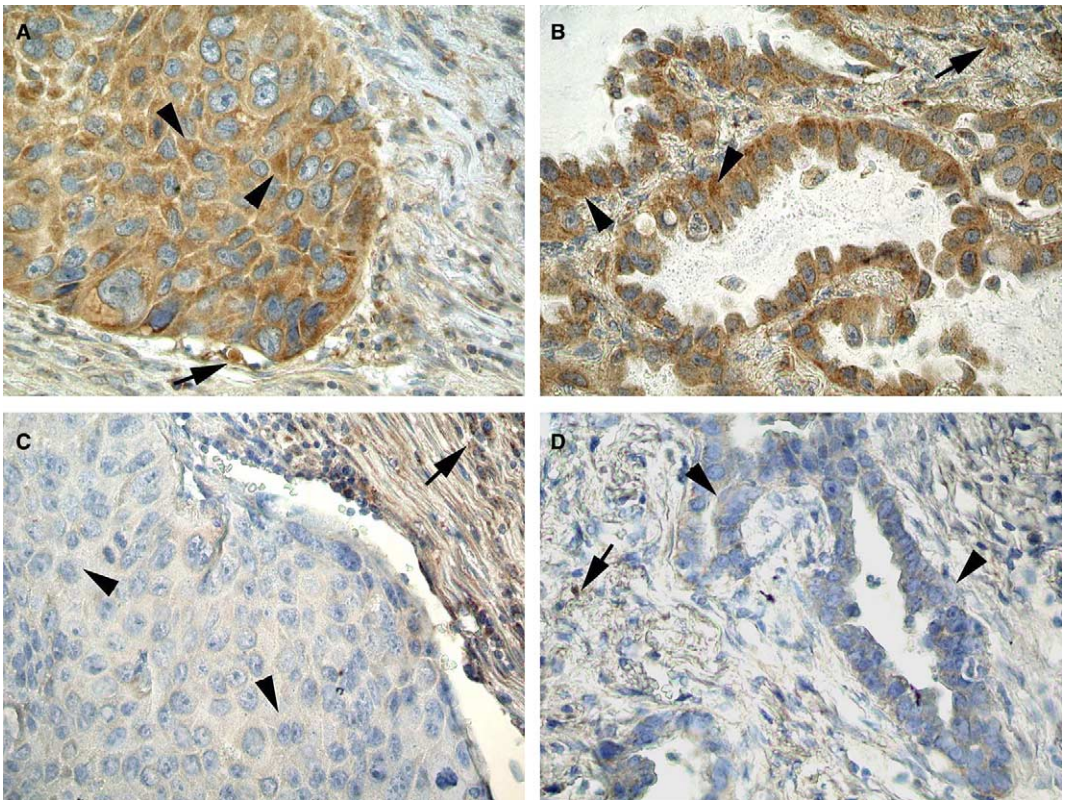

Fig. 1. Immunohistochemical analysis of Fhit in formalin-fixed paraffin-embedded sections of resected tumour specimens of the lung. Cytoplasmic immunoreactivity is considered positive and is visible as a brown precipitate. Positive immunoreactivity in stromal cells (*arrows*) of resected tumour specimens serves as an internal control. SQ (A) and AD tumours (B) showed positive staining (*arrowheads*). No immunoreactivity was visible in SQ (C) or AD tumours (D) (*arrowheads*). (Original magnification 200×).

Table 1
Alterations in the *FHIT* gene in relation to clinicopathological parameters of resected primary NSCLC

Characteristics	Protein expression			mRNA expression			Promoter methylation			LOH		
	Total	+	–[a] (%)	Total	+	–[a] (%)	Total	–	+[a] (%)	Total	–	+[a] (%)
Overall[b]	129	64	65 (50)	98	60	38 (39)	91	63	28 (31)	64 (44)[c]	30	14 (32)
Age (mean ± SD)		62 ± 11	65 ± 11		65 ± 10	64 ± 12		64 ± 10	65 ± 11		63 ± 14	64 ± 10
Gender												
Male	110	54	56 (51)	82	48	34 (42)	74	49	25 (34)	36	22	14 (39)[g]
Female	19	10	9 (47)	16	12	4 (25)	17	14	3 (18)	8	8	0 (0)
Smoking status												
Smoker	97	46	51 (53)	72	43	29 (40)	66	45	21 (32)	33	21	12 (36)
Non-smoker	32	18	14 (44)	26	17	9 (35)	25	18	7 (28)	11	9	2 (18)
Tumour type												
SQ	68	21	47 (69)[d]	51	26	25 (49)[e]	44	26	18 (41)[f]	26	14	12 (46)[h]
AD	54	39	15 (28)	40	28	12 (30)	40	30	10 (25)	17	16	1 (6)
AS	3	2	1 (33)	3	3	0 (0)	3	3	0 (0)	0	0	0 (0)
LC	4	2	2 (50)	4	3	1 (25)	4	4	0 (0)	1	0	1 (100)
Tumour stage												
I + II	66	31	35 (53)	52	31	21 (40)	46	29	17 (37)	27	16	11 (41)
III + IV	63	33	30 (48)	46	30	16 (35)	45	34	11 (24)	17	14	3 (18)

SD, Standard Deviation.
[a] These groups represent patients with alteration in the *FHIT* gene/protein. Alteration in mRNA expression includes samples with low or aberrant transcripts of *FHIT* gene.
[b] Total number of samples in some categories is less than the overall number analysed because some samples were not assayed for the alteration.
[c] Of the 64 samples analysed, 44 were informative cases that showed two distinguishable alleles of different sizes in the normal DNA.
[d] $P < 0.0001$ between SQ and AD by Pearson's χ^2 test.
[e] $P = 0.068$ between SQ and AD by Pearson's χ^2 test.
[f] $P = 0.122$ between SQ and AD by Pearson's χ^2 test.
[g] $P = 0.030$ by Pearson's χ^2 test.
[h] $P = 0.007$ between SQ and AD by Pearson's χ^2 test.

samples with aberrant *FHIT* transcripts (data not shown).

3.3. FHIT 5′CpG hypermethylation in primary NSCLC tumours and matched bronchial biopsies

Alternative splicing of *FHIT* transcripts only partly explains the mechanisms underlying the frequent aberrant expression of Fhit in our patients. Therefore, we studied 5′CpG hypermethylation of the *FHIT* gene using an MSP assay in this cohort of NSCLC (Fig. 3A). As shown in Table 1, 31% (28/91) of lung tumours showed hypermethylation of the exon 1 region of the *FHIT* gene. In addition, the methylation status of 12 bronchial biopsy samples was analysed in parallel with the analyses of resected lung tumours (Fig. 3B). Promoter hypermethylation of the *FHIT* gene was found in 6/12 biopsy specimens collected 1–6 months before surgery. Notably, an 83% (10/12) concordance in the methylation status of *FHIT* was demonstrated between bronchial biopsy samples and their matched resected tumours. Three bronchial specimens, which contained mild dysplasia or moderate dysplasia lesions, did indeed show loss of Fhit protein expression (data not shown). However, the other three methylation-positive samples were cytologically negative and did not show aberrant protein expression. Nevertheless, aberrant protein and methylation status could be detected in their tumour samples obtained 6 months later.

3.4. Concordance analysis of FHIT methylation, mRNA expression and protein expression

A subset of 81 tumours was examined using all of the analyses, including protein and mRNA expression and DNA methylation. These data were then cross-referenced to investigate the correlations between these three parameters (Fig. 4). Aberrant Fhit protein expression was significantly associated with aberrant *FHIT* mRNA expression ($P < 0.0001$) and with 5′CpG hypermethylation of the *FHIT* gene ($P = 0.0001$). Furthermore, aberrant *FHIT* mRNA expression was significantly associated with hypermethylation of the *FHIT* gene ($P < 0.0001$).

3.5. LOH at D3S1234 in resected tumours and contribution of promoter hypermethylation, aberrant splicing and LOH to biallelic inactivation of FHIT

The highly variable frequency of LOH at the *FHIT* locus reported previously for NSCLC may be due to the use of various microsatellite markers relatively

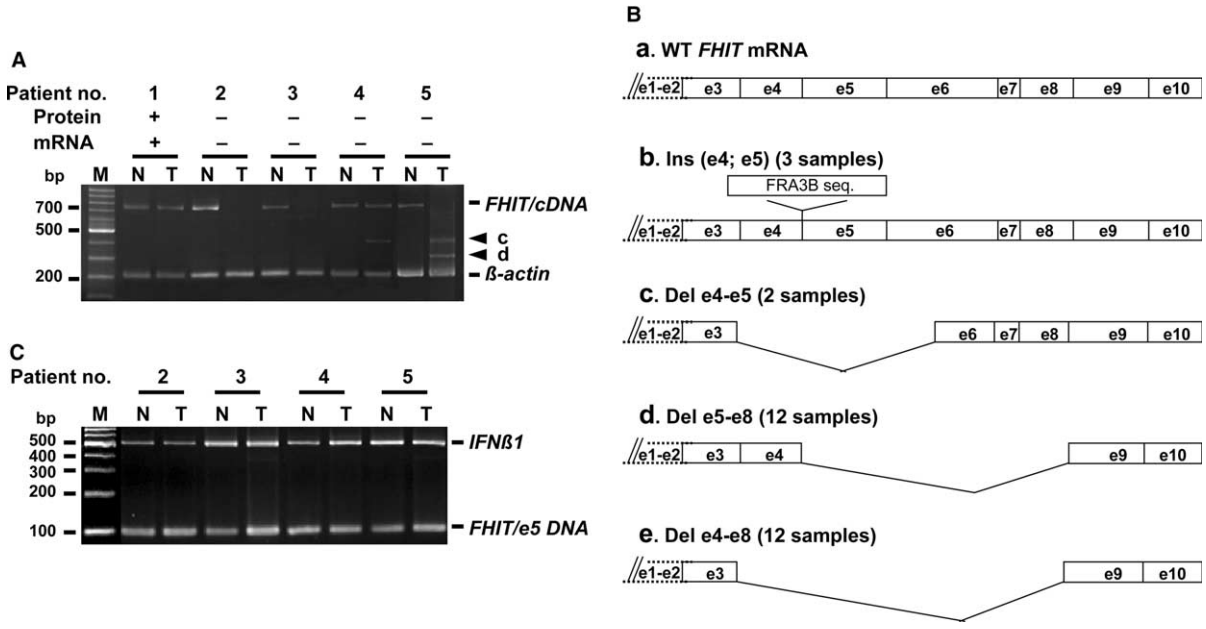

Fig. 2. Representative figures for mRNA expression analysis (A), the spectrum of aberrant splicing in all samples analysed (B), and genomic exon 5 analyses (C). *N*, normal lung tissue; *T*, tumour tissue of the lung. (A) Patients 2, 3, and 5 were negative for *FHIT* mRNA expression. Patients 4 and 5 expressed smaller-sized products (*arrows c and d*) and their aberrant splicing patterns are described in (B). (B) describes the spectrum of aberrant splicing in all samples analysed. The wild-type cDNA sequence is shown in panel *a*. The insertion of a 197-bp fragment between exons 4 and 5 was demonstrated in three samples (panel *b*). Panel *c* illustrates the three samples in which exons 4 and 5 were completely absent, as were the first 88 base pairs of exon 6, leaving a residual exon 6, which starts at nucleotide 554. Aberrant transcripts often showed a loss of exons 5–8 or exons 4–8, as shown in panels *d* and *e*, respectively. (C) is the representative figure of genomic exon 5 deletion analysis in the *FHIT* gene. These four patients had no exon 5 deletion in their genomic DNA, although they showed low expression of *FHIT* mRNA.

distant from the gene. Therefore, microdissected genomic DNA obtained from 64 available matched pairs of primary tumours and nearby normal lung tissue was examined for the incidence of LOH at the intragenic microsatellite marker, D3S1234. Fig. 5 shows representative results of the LOH analysis. Fourteen (32%) of the 44 informative cases were found to harbour LOH at the D3S1234 microsatellite marker (Table 1). The incidence of LOH at D3S1234 was significantly higher in SQ tumours than in AD tumours ($P=0.007$), although the numbers are small. LOH at the *FHIT* locus also occurred more frequently in tumours from male patients than in those from female patients ($P=0.03$). LOH at D3S1234 tended to be more frequently associated with patients without Fhit protein expression than patients with Fhit protein expression, although the trend was non-significant ($P=0.342$).

The two-step biallelic inactivation process could be reflected by the LOH of polymorphic markers linked to the suppressor gene locus and its correlation with other alterations. Eight samples with no expression of Fhit protein clearly showed the retention of both alleles and DNA hypermethylation, indicating that biallelic inactivation of Fhit expression was induced by 5′CpG hypermethylation. Five samples with no expression of Fhit protein showed aberrant size of transcripts, indicating that biallelic inactivation of Fhit expression was induced by alternative mRNA expression. Three samples lacking Fhit expression, but exhibiting aberrant splicing and LOH in the *FHIT* gene, suggest that biallelic inactivation of the *FHIT* gene resulted from the loss of one allele and aberrant splicing in the remaining allele. Note that five samples with no expression of Fhit protein clearly showed the retention of both alleles, alternative mRNA splicing, and DNA hypermethylation, indicating that biallelic inactivation of Fhit expression was induced by alternative splicing of one allele and 5′CpG hypermethylation in the other allele.

4. Discussion

In this study, a comprehensive genetic and epigenetic analysis of the patterns of inactivation of the *FHIT* gene was conducted using 129 primary NSCLC tumours. Immunohistochemical analysis showed aberrant Fhit expression in 50% of 129 patients with NSCLC. To elucidate the possible molecular mechanisms responsible for this loss of protein expression, we used RT-PCR and cDNA sequencing analyses of *FHIT* transcripts and MSP for 5′CpG hypermethylation of *FHIT* gene. A highly significant correlation was observed between aberrant protein expression and alternative splicing, as well as between aberrant protein expression and hyper-

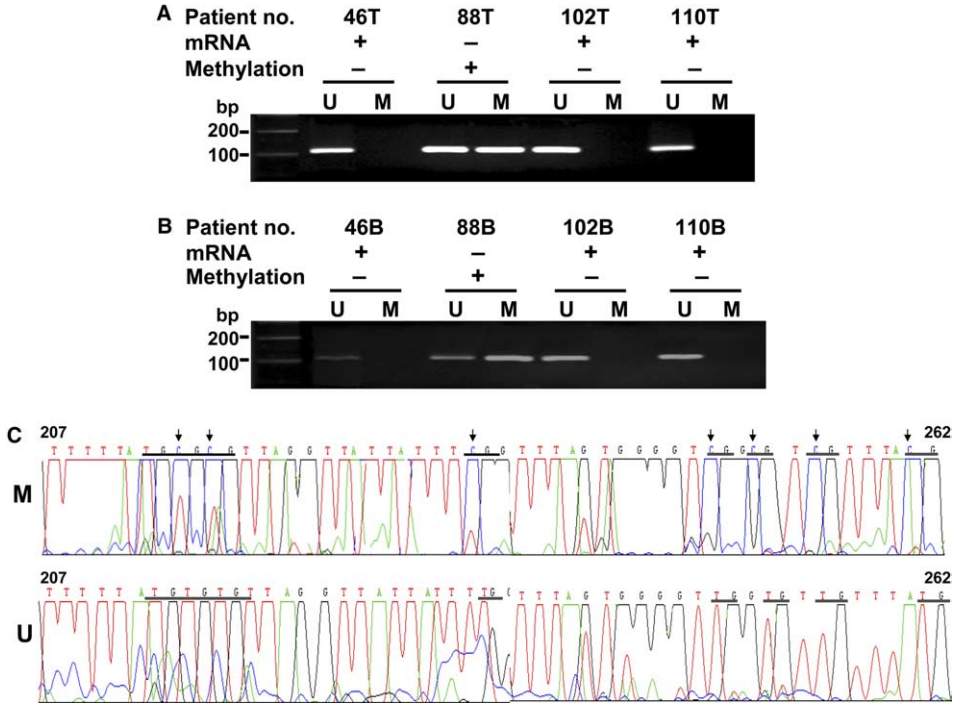

Fig. 3. Representative figures of the MSP assay and bisulphite sequencing assay. (A) shows the results for four samples of lung tumours, and the results for their matched bronchial samples are shown in (B). Tumour samples and matched bronchial samples are indicated by T and B, respectively, after the subject identification number. The primer sets used for amplification are designated "U" for unmethylated or "M" for methylated genes. + (positive) and – (negative) in the rows labelled "Methylation" and "mRNA" indicate the status of DNA methylation and mRNA expression. Promoter methylation in tumour samples was concordant with promoter methylation in bronchial biopsy samples in all four patients. (C) is representative of *FHIT* bisulphite sequencing analysis in the region between nucleotides 207 and 262.

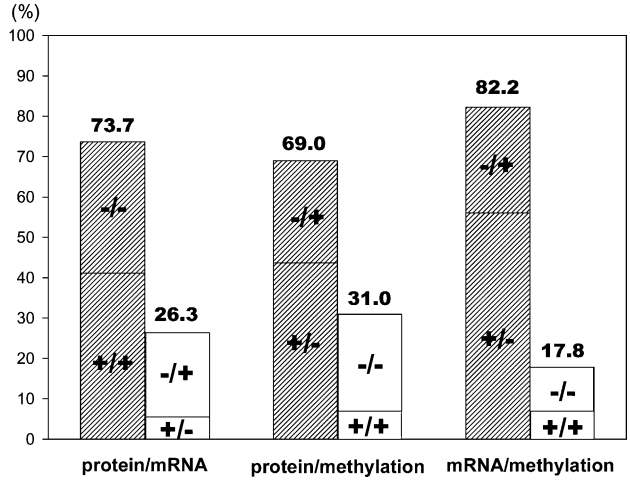

Fig. 4. Concordance analysis between protein expression, mRNA expression, and promoter methylation of the *FHIT* gene. The percentage of cases is indicated on the *Y*-axis, whereas the type of comparison is plotted on the *X*-axis. "+" indicates positive protein expression, positive mRNA expression and DNA hypermethylation, as opposed to "–", which indicates a negative result. Numbers above the bars indicate the percentage in the total concordant group (gray section) and non-concordant group (white section).

methylation of *FHIT*. Allelic inactivation data suggest that DNA hypermethylation and mRNA splicing changes are both predominant mechanisms leading to *FHIT* deregulation. To our knowledge, the analyses on the 5′CpG hypermethylation and aberrant mRNA splicing in the same series of cancer patients to reveal their contribution to *FHIT* inactivation has not been reported. This is also one of the few studies to show the presence of promoter hypermethylation in primary tumours and bronchial lesions in lung cancer.

5′CpG hypermethylation is the major epigenetic modification of mammalian genomes during development and is involved in gene inactivation of tumour suppressor genes during tumorigenesis [24]. Methylation of a 5′CpG island that leads to gene silencing of the *FHIT* has been described in oesophageal cancer [13] and breast cancer [25], but reports are quite limited regarding primary lung cancers [22,26]. Zöchbauer-Müller and colleagues [22] reported that CpG-island methylation of *FHIT* occurs in 37% of primary lung tumours and is distributed most frequently in the region between nucleotides 195 and 283. Using an approach of MSP followed by genomic sequencing of the 5′CpG island after bisulphite treatment, we also observed frequent *FHIT* methylation in the region between nucleotides 207 and 262 (Fig. 3C). It will be important to examine in the future the methylation status of all CpG sites within a much larger region to define more precisely the critical site for gene silencing. By taking advantage of sensitive molecular techniques, we were able to study

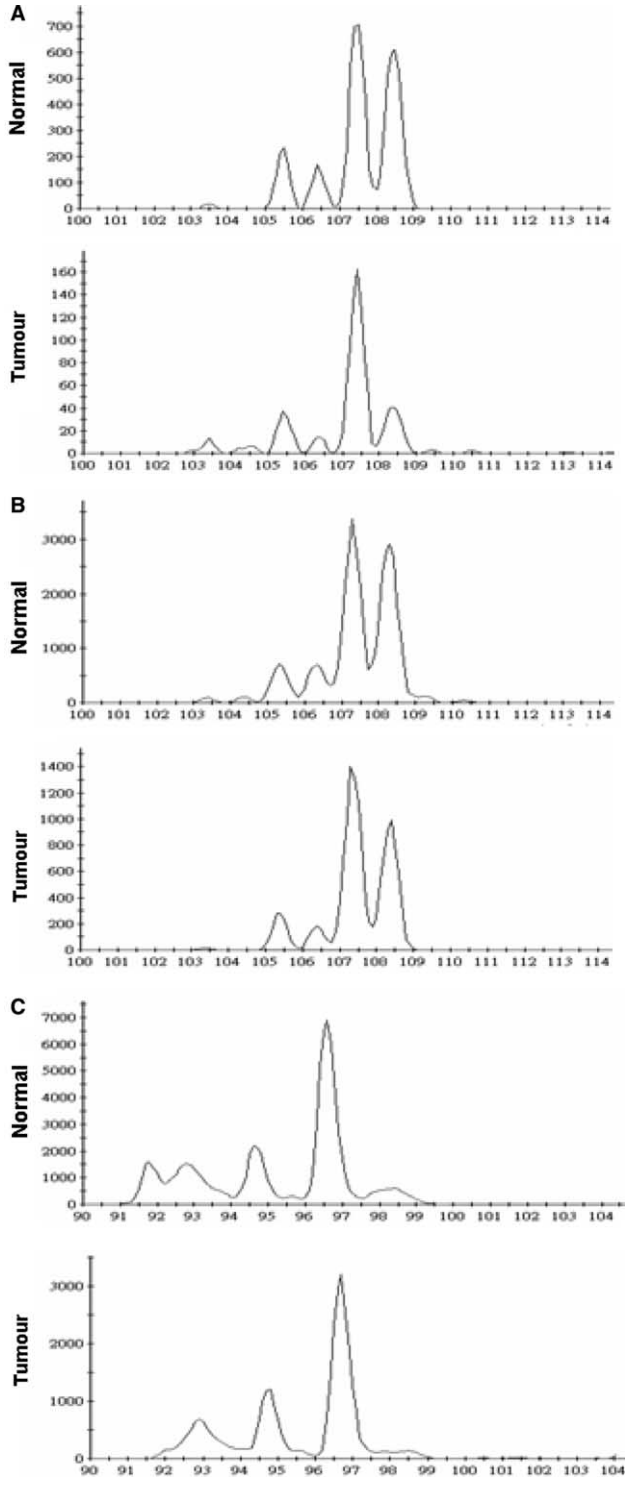

Fig. 5. Representative figures for the detection of LOH at the D3S1234 microsatellite marker in microdissected DNA from (A) an LOH patient, (B) a heterozygous patient, and (C) a non-informative patient. PCR products from tumour and normal lung DNA were compared. The number on the *X*-axis indicates the length of the fragment, and the number on the *Y*-axis shows the fluorescence intensity of peak area.

DNA hypermethylation in bronchial precancerous lesions. We demonstrated an 83% (10/12) concordance in the methylation status of *FHIT* between bronchial biopsy samples collected before surgery and their matched resected tumours. Three methylation-positive samples were cytologically negative and did not show aberrant protein expression. Nevertheless, aberrant protein and methylation status could be detected in their tumour samples obtained 6 months later. The data suggested that *FHIT* promoter methylation may occur before loss of protein expression. These results are in a general agreement with the data from previous reports by Zöchbauer-Müller and colleagues [22], who showed *FHIT* 5′CpG methylation in 17% of 35 samples of bronchial brushes from chronic smokers. More comprehensive mechanistic molecular study needs to be strengthened by further investigations in a larger cohort of patients.

In RT-PCR analysis, 38 patients with NSCLC exhibited low or absent *FHIT* mRNA expression. Of these, 24 patients showed transcripts of abnormal sizes and several samples contained more than one transcript of varying sizes. Sequencing of the abnormally-sized cDNA products suggested that these were most likely attributable to errors in the splicing of pre-mRNA. Most alternative splicing products of the *FHIT* gene were lacking exons 5–8 or exons 4–8, and exon 5 was the most frequently deleted exon (Fig. 2). To examine whether aberrant transcripts resulted from deletions in the genomic *FHIT* gene, we analysed a subset of 20 genomic DNA samples from patients with aberrantly-sized transcripts for the deletion of exon 5, using a multiplex-PCR assay (Fig. 2C). None of the genomic DNA samples showed a deletion of exon 5, thus providing evidence that the aberrant *FHIT* transcripts are not caused by a deletion of the genomic sequence of *FHIT*. This is consistent with data obtained previously by others [18,21], suggesting that the frequent lack of exons 4–8 and 5–8 in *FHIT* cDNA is predominantly due to splicing abnormalities. Interestingly, two samples showed a lack of exon 4 and exon 5, as well as a lack of the first 88 bp of exon 6, leaving a residual exon 6 starting from nucleotide 554 (Fig. 2B). The sequence of nucleotides 552 and 553 is AG, which may serve as a cryptic 3′ intron junction during splicing. Three samples contained a 197-bp insertion between exon 4 and exon 5, the alteration sites of which did not conform to the GT–AG splicing rule. After alignment with the DNA sequences in GenBank, the inserted fragment was identified as part of the *FRA3B* genomic sequence (Fig. 2B).

In many cancers, biallelic inactivation of tumour suppressor genes is observed [25]. This two-step process is reflected by the LOH of polymorphic markers linked to the suppressor gene locus. We looked for such LOH at the D3S1234 marker in the *FHIT* gene and examined its correlation with the status of aberrant splicing and 5′CpG hypermethylation. Eight samples showed biallelic inactivation of Fhit expression by 5′CpG hypermethylation. Five samples showed biallelic

inactivation by alternative mRNA expression. Note that five samples showed biallelic inactivation of Fhit expression by alternative splicing of one allele and 5′CpG hypermethylation in the other allele. Allelic inactivation data suggest that biallelic inactivation of *FHIT* by 5′CpG hypermethylation and splicing alterations could lead to the complete inactivation of *FHIT* gene in patients with NSCLC.

In conclusion, of a subset of patients in whom we were able to analyse all different types of *FHIT* aberration, 60% displayed at least one type of molecular alteration in gene expression, indicating that *FHIT* deregulation is involved in NSCLC tumorigenesis. We observed more frequent changes in *FHIT* expression in lung SQ than in lung AD. This is similar to data reported by Geradts and colleagues [19] and by Sozzi and colleagues [23]. These results suggest that these changes in *FHIT* expression play a more significant role in the development of lung SQ than in AD. Our results also indicate a good correlation between DNA hypermethylation of, and mRNA and protein expression from, the *FHIT* gene, suggesting that 5′CpG hypermethylation and alternative splicing of mRNA transcripts are two major molecular mechanisms responsible for aberrant Fhit protein expression. Significant concordance between *FHIT* methylation status was observed between resected tumours and matched bronchial samples. These results imply a possible role for *FHIT* methylation as a molecular diagnostic method of NSCLC in conjunction with conventional bronchoscopic cytology.

Conflict of interest

None.

References

1. Ohta M, Inoue H, Cotticelli MG, *et al*. The FHIT gene, spanning the chromosome3p14.2 fragile site and renal carcinoma-associated (3;8) breakpoint, is abnormal in digestive tract cancers. *Cell* 1996, **84**, 587–597.
2. Huebner K, Garrison PN, Barnes LD, Croce CM. The role of the FHIT/FRA3B locus in cancer. *Annu Rev Genet* 1998, **32**, 7–31.
3. Mimori K, Druck T, Inoue H, *et al*. Cancer-specific chromosome alterations in the constitutive fragile region FRA3B. *Proc Natl Acad Sci USA* 1999, **96**, 7456–7461.
4. Garinis GA, Gorgoulis VG, Mariatos G, *et al*. Association of allelic loss at the FHIT locus and p53 alterations with tumour kinetics and chromosomal instability in non-small cell lung carcinomas (NSCLCs). *J Pathol* 2001, **193**, 55–65.
5. Mao L. Tumour suppressor genes: Does FHIT fit. *J Natl Cancer Inst* 1998, **90**, 412–414.
6. Otterson GA, Xiao GH, Geradts J, *et al*. Protein expression and functional analysis of the FHIT gene in human tumour cells. *J Natl Cancer Inst* 1998, **90**, 426–432.
7. Zanesi N, Fidanza V, Fong LY, *et al*. The tumour spectrum in FHIT-deficient mice. *Proc Natl Acad Sci USA* 2001, **98**, 10250–10255.
8. Ji L, Fang B, Yen N, Fong K, Minna JD, Roth JA. Induction of apoptosis and inhibition of tumorigenicity and tumour growth by adenovirus vector-mediated fragile histidine triad (FHIT) gene overexpression. *Cancer Res* 1999, **59**, 3333–3339.
9. Dumon KR, Ishii H, Fong LY, *et al*. FHIT gene therapy prevents tumour development in Fhit-deficient mice. *Proc Natl Acad Sci USA* 2001, **98**, 3346–3351.
10. Negrini M, Monaco C, Vorechovsky I, *et al*. The FHIT gene at 3p14.2 is abnormal in breast carcinomas. *Cancer Res* 1996, **56**, 3173–3179.
11. Ahmadian M, Wistuba II, Fong KM, *et al*. Analysis of the FHIT gene and FRA3B region in sporadic breast cancer, preneoplastic lesions, and familial breast cancer probands. *Cancer Res* 1997, **57**, 3664–3668.
12. Mandai M, Konishi I, Kuroda H, *et al*. Expression of abnormal transcripts of the FHIT (fragile histidine triad) gene in ovarian carcinoma. *Eur J Cancer* 1998, **34**, 745–749.
13. Tanaka H, Shimada Y, Harada H, *et al*. Methylation of the 5′CpG island of the FHIT gene is closely associated with transcriptional inactivation in esophageal squamous cell carcinomas. *Cancer Res* 1998, **58**, 3429–3434.
14. Sozzi G, Veronese ML, Negrini M, *et al*. The FHIT gene 3p14.2 is abnormal in lung cancer. *Cell* 1996, **85**, 17–26.
15. Fong KM, Biesterveld EJ, Virmani A, *et al*. FHIT and FRA3B 3p14.2 allele loss are common in lung cancer and preneoplastic bronchial lesions and are associated with cancer-related FHIT cDNA splicing aberrations. *Cancer Res* 1997, **57**, 2256–2267.
16. Sozzi G, Sard L, De Gregorio L, *et al*. Association between cigarette smoking and FHIT gene alterations in lung cancer. *Cancer Res* 1997, **57**, 2121–2123.
17. Burke L, Khan MA, Freedman AN, *et al*. Allelic deletion analysis of the FHIT gene predicts poor survival in non-small cell lung cancer. *Cancer Res* 1998, **58**, 2533–2536.
18. Sozzi G, Tornielli S, Tagliabue E, *et al*. Absence of Fhit protein in primary lung tumours and cell lines with FHIT gene abnormalities. *Cancer Res* 1997, **57**, 5207–5212.
19. Geradts J, Fong KM, Zimmerman PV, Minna JD. Loss of Fhit expression in non-small-cell lung cancer: correlation with molecular genetic abnormalities and clinicopathological features. *Br J Cancer* 2000, **82**, 1191–1197.
20. Tseng JE, Kemp BL, Khuri FR, *et al*. Loss of Fhit is frequent in stage I non-small cell lung cancer and in the lungs of chronic smokers. *Cancer Res* 1999, **59**, 4798–4803.
21. Tokuchi Y, Kobayashi Y, Hayashi S, *et al*. Abnormal FHIT transcripts found in both lung cancer and normal lung tissue. *Genes Chromosomes Cancer* 1999, **24**, 105–111.
22. Zöchbauer-Müller S, Fong KM, Maitra A, *et al*. 5′CpG island methylation of the FHIT gene is correlated with loss of gene expression in lung and breast cancer. *Cancer Res* 2001, **61**, 3581–3585.
23. Sozzi G, Pastorino U, Moiraghi L, *et al*. Loss of FHIT function in lung cancer and preinvasive bronchial lesions. *Cancer Res* 1998, **58**, 5032–5037.
24. Baylin SB, Herman JG. DNA methylation in tumorigenesis: epigenetics joins genetics. *Trends Genet* 2000, **16**, 168–174.
25. Yang Q, Nakamura M, Nakamura Y, *et al*. Two-hit inactivation of FHIT by loss of heterozygosity and hypermethylation in breast cancer. *Clin Cancer Res* 2002, **8**, 2890–2893.
26. Maruyama R, Sugio K, Yoshino I, *et al*. Hypermethylation of FHIT as a prognostic marker in nonsmall cell lung carcinoma. *Cancer* 2004, **100**, 1472–1477.